Growth of ZrSnTiO thin films by pulsed-laser deposition

2007 J. Phys.: Condens. Matter 19 096006

(http://iopscience.iop.org/0953-8984/19/9/096006)

IOP PUBLISHING JOURNAL OF PHYSICS: CONDENSED MATTER

J. Phys.: Condens. Matter **19** (2007) 096006 (16pp) doi:10.1088/0953-8984/19/9/096006

Growth of ZrSnTiO thin films by pulsed-laser deposition

M Nistor[1], A Ioachim[2], B Gallas[3], D Defourneau[3], J Perrière[3] and W Seiler[4]

[1] National Institute for Lasers, Plasma and Radiation Physics, PO Box MG-36, 77125 Bucharest-Magurele, Romania
[2] National Institute for Material Physics, PO Box MG-5, 77125 Bucharest-Magurele, Romania
[3] Université Pierre et Marie Curie-Paris6, CNRS UMR 7588, INSP, Campus Boucicaut, 140 rue de Lourmel, 75015 Paris, France
[4] LIM, UMR CNRS 8006, ENSAM, 151, Boulevard de l'Hôpital, 75013 Paris, France

E-mail: mnistor@infim.ro

Received 5 September 2006, in final form 4 December 2006
Published 12 February 2007
Online at stacks.iop.org/JPhysCM/19/096006

Abstract

The formation of ZrSnTiO thin films by pulsed-laser deposition has been studied. By the complementary use of Rutherford backscattering spectrometry, x-ray diffraction and scanning electron microscopy, the composition, crystalline structure and surface morphology of the films were investigated. The optimum conditions for the growth of dense, stoichiometric and crystalline films were determined, i.e. substrate temperature of 700 °C and oxygen pressure in the 10^{-3}–0.1 mbar range. Such ZrSnTiO films present the classical orthorhombic structure for growth on Si substrates, while the use of MgO single crystal substrates leads to the formation of epitaxial ZrSnTiO films with a tetragonal structure. This previously unobserved ZrSnTiO crystalline phase obtained in thin film form is the result of an epitaxy stabilization effect, and presents improved optical properties as shown by the results of spectroscopic ellipsometry measurements. Moreover, the films grown at 700 °C under low oxygen pressure ($<10^{-5}$ mbar) were composed of a Sn rich surface layer superimposed on an understoichiometric zirconium titanate oxide film near the substrate. This last layer, which crystallizes in a cubic structure and has never been reported in bulk material, could be related to the presence of oxygen vacancies in the films grown in these conditions.

(Some figures in this article are in colour only in the electronic version)

1. Introduction

Ceramics based on zirconium tin titanate solid solutions with up to 20 at.% of Zr replaced by Sn present a high dielectric constant in the microwave frequency range, a high quality factor and a low temperature coefficient of resonant frequency [1–3]. Owing to these specific physical properties, bulk zirconium tin titanate $Zr_xSn_yTi_zO_4$ (ZST) has been extensively studied for applications in various domains, like resonators, phase shifters and filters in mobile communications. A large number of publications on bulk ZST are thus available, but only a few studies of ZST thin films have been reported, although this material is considered as a valuable high k dielectric candidate to replace silicon dioxide in future semiconductors [4].

Various deposition techniques have been used to obtain ZST thin films: RF magnetron sputtering [5–7], chemical vapour deposition [8], pulsed-laser deposition [9–11] and pulsed electron beam deposition [12]. These works are generally focused on the physical properties of the films, and show that the formation of crystalline ZST thin films substantially improves their dielectric properties by comparison with amorphous thin films, and that crystallization of (Zr, Sn) TiO_4 thin films needs either substrate temperatures higher than 500 °C during deposition under oxygen partial pressure [9] or a post-deposition thermal annealing treatment [7]. However, precise information on the cationic composition and oxygen stoichiometry of the ZST films is not given in these works; the sole point which is sometimes mentioned is that compared to the nominal composition of the target a deficiency of the tin is observed due to its volatility for temperatures higher than 300 °C under low oxygen pressures. Moreover, it is generally claimed in the literature that the ZST thin films crystallize in the expected orthorhombic structure of the bulk material, but the values of the lattice parameters are not given. Finally, to the best of our knowledge, the formation of epitaxial ZST thin films on single crystal substrates has not been reported in the literature.

The main problem in the growth of complex oxides are composition deviations which can lead to the formation of spurious phases with a high level of structural defects. As a result the functional dielectric properties of such thin films can be very different from those of the bulk material. A detailed knowledge of the composition and nature of the crystalline phases present in thin films of complex materials is thus needed, in conjunction with the growth conditions. This is the main objective of this work in the case of ZrSnTiO thin films grown by pulsed-laser deposition (PLD). As this material is a complex multicomponent oxide, a congruent method for thin film growth has to be envisaged. PLD is considered to be a congruent method leading to oxide films presenting the composition of the target [13]. In this work, various techniques were used to determine the composition, structure and surface morphology of the ZrSnTiO films as a function of the PLD conditions, and these characteristics were correlated with their optical properties. Moreover, the use of MgO single crystal substrates leads to the growth of epitaxial ZST films with crystalline structures depending upon the growth conditions. As a result, previously unobserved zirconium titanate crystalline phases have been obtained in thin film form, via the epitaxial stabilization effect.

2. Experimental details

Thin films of ZrSnTiO were grown by PLD on various substrates: amorphous SiO_2 thermally grown on Si substrates, (100) oriented Si and MgO single crystals and c-cut sapphire. Details of the PLD method are given elsewhere [14]. Briefly, PLD was performed using a pulsed Nd:YAG laser delivering pulses of 7 ns duration at a 5 Hz repetition rate with an energy of 2 J at the fundamental 1.064 μm wavelength. Fourth harmonic generation (266 nm) was obtained using frequency doubling crystals. The ZrSnTiO target, placed in the ablation chamber, was irradiated

by pulses in the 50–500 MW cm^{-2} range at a 45° angle of incidence. The $Zr_{0.8}Sn_{0.2}TiO_4$ target was prepared via a conventional solid-state reaction method from oxide powders (ZrO_2, SnO_2, TiO_2) with purity higher than 99.9% and with 2 wt% La_2O_3 and 1 wt% ZnO added as sintering additives. These ZST ceramic targets were previously characterized in the microwave range [3]. The ZrSnTiO thin films were grown under controlled substrate temperatures (from room temperature to 700 °C) and oxygen pressures (from 0.1–10^{-6} mbar). After deposition, the films were cooled down in the ablation chamber under the oxygen pressure conditions used for the growth process.

The thickness and composition of the films were determined by Rutherford backscattering spectrometry (RBS), using the 2 MeV van de Graaff accelerator of the INSP. The precise in-depth distribution of the various atomic constituents of the films was obtained by the use of the RUMP simulation program [15]. Such measurements gave a composition determination for the cations (Zr, Sn and Ti) with a rather good precision (±2%), while the oxygen content was only determined with a 5% precision, owing to the low RBS yield on light elements like oxygen. The oxygen content of the films was specifically studied by nuclear reaction analysis (NRA) by the direct observation of the protons emitted during the $^{16}O(d, p)^{17}O^*$ nuclear reaction induced by a 850 keV deuteron beam [16]. The absolute number of oxygen atoms in the films was obtained by comparison with an oxygen reference target known to within ±3% [16]. The crystalline structure of the films was studied by x-ray diffraction analyses (XRD) using a Philips Xpert diffractometer. The nature of the crystalline phases was determined by diffraction either in the Bragg–Brentano mode or in the grazing incidence geometry. The epitaxial relationships between ZST films and single crystal substrates were studied by asymmetric diffraction. The surface morphology of the films was studied by scanning electron microscopy (SEM).

The optical properties of the films were studied by spectroscopic ellipsometry using a SOPRA rotating polarizer ellipsometer. Ellipsometry measures the complex reflectivity ratio of the light in p- and s-polarization as $\frac{r_p}{r_s} = |\frac{r_p}{r_s}| \exp(-i(\delta_p - \delta_s)) = \tan(\Psi)\cos(\Delta)$, where $\Delta = \delta_p - \delta_s$ is the phase shift difference between p- and s-polarization introduced by the reflection. Measurements were carried out at incidence angles of 65° and 75° as a function of the photon energy in the 1.6–6 eV range. The use of these two incidence angles ensured a good sensitivity to the variations of the measured parameters in the whole spectral range.

3. Results

3.1. Film composition

It is generally admitted that laser ablation yields films with a composition close to that of the target, even in the case of complex materials [13]. However, composition deviations have already been reported during PLD of various polycationic oxides [16]. The origin of these composition deviations can be found in the phenomena occurring during the growth by PLD (broadening of the angular distribution of the various species during the plume expansion), or in the material itself by the presence of volatile species.

Rutherford backscattering spectrometry was used to study the composition of the ZST thin films grown at various temperatures and oxygen pressures. Figures 1 and 2 show typical RBS spectra of ZST thin films grown for two oxygen pressures (0.1 and 10^{-6} mbar) and two temperatures (room temperature and 700 °C). The film grown at 700 °C under 0.1 mbar oxygen pressure shows a clear Zr enrichment and Ti depletion with respect to the composition of the target (figure 1(a)), i.e. $Zr_{1.08}Sn_{0.25}Ti_{0.92}$ in the film and $Zr_{0.8}Sn_{0.2}Ti_1$ in the target. Uniform in-depth distributions for the various elements are deduced from the RUMP simulation, without any interdiffusion between the film and the Si substrate as shown by the sharp front edge of

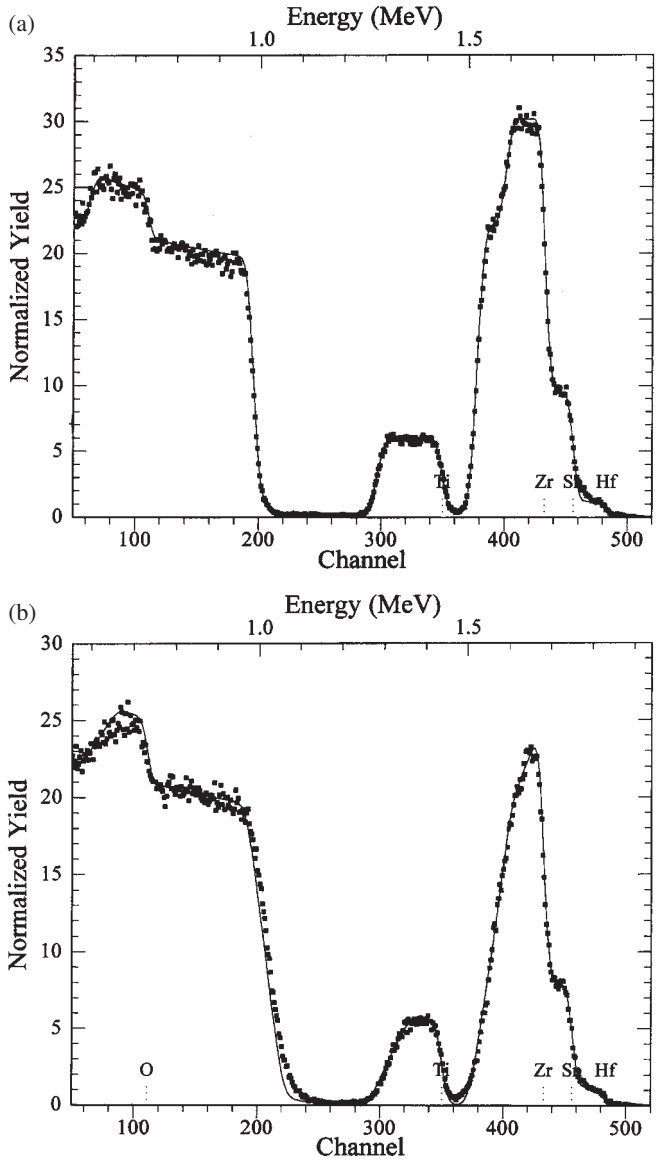

Figure 1. RBS spectra for films grown under 0.1 mbar oxygen pressure at (a) 700 °C and (b) room temperature. The solid lines correspond to the best fit of the spectra calculated with the RUMP simulation program.

the Si contribution and rear edges of the contribution of each element of the film. These points also mean that smooth films are grown in these conditions. Identical results were obtained with SiO_2 on Si, Al_2O_3 or MgO substrates. The ZST films prepared under 0.1 mbar oxygen pressure were found to be stoichiometric. Indeed the ratio of the oxygen (determined by NRA) to overall cationic content (deduced from the RBS analysis) was found to be equal to 2 (the ideal value deduced from the valence of cations) within the experimental precision (±5%). A slight decrease in this ratio was observed in the films grown in 0.1–10^{-3} mbar oxygen pressure, indicating a decrease in the amount of oxygen incorporated into the films.

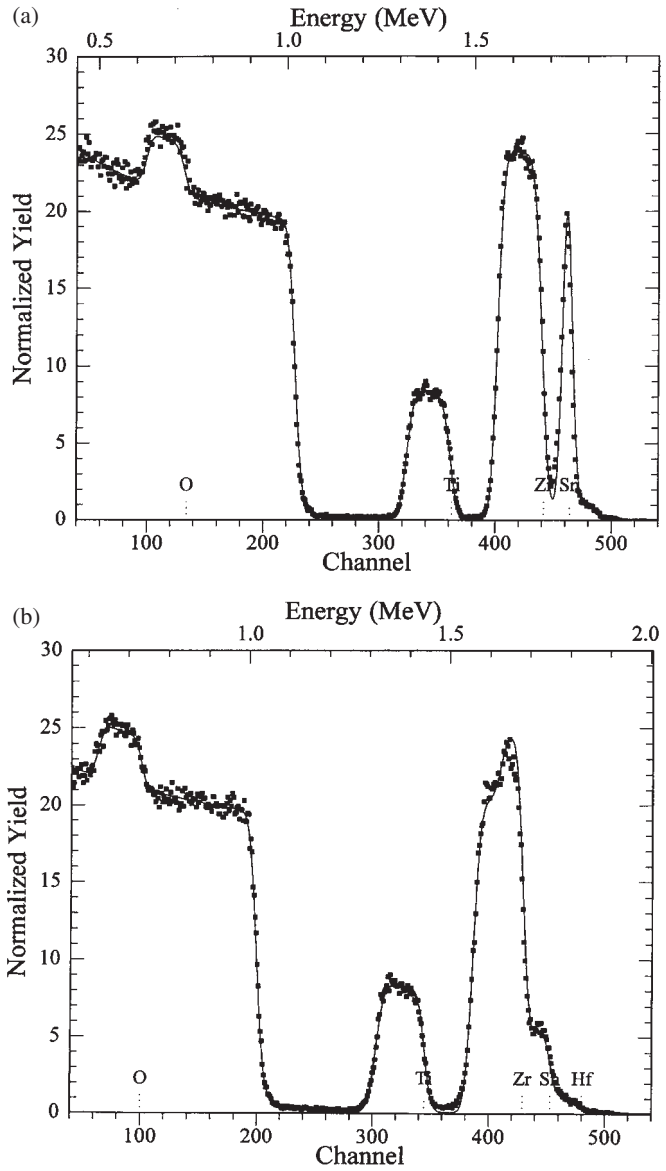

Figure 2. RBS spectra for films grown under 10^{-6} mbar oxygen pressure at (a) 700 °C and (b) room temperature. The solid lines correspond to the best fit of the spectra calculated with the RUMP simulation program.

A decrease of the substrate temperature (figure 1(b)) leads to the presence of tails towards lower energies on the RBS contribution of each element of the film and to a large broadening of the front edge of the Si substrate contribution. This particular shape of the RBS spectrum cannot be explained by film–substrate interdiffusion (the growth occurs at room temperature). It is due to a significant surface roughness of the film. In fact, at low (room) temperature, the mobility of the species at the surface of the substrate is rather low, and this leads to an island type of growth with a high density of nucleation centres, which is at the origin of the

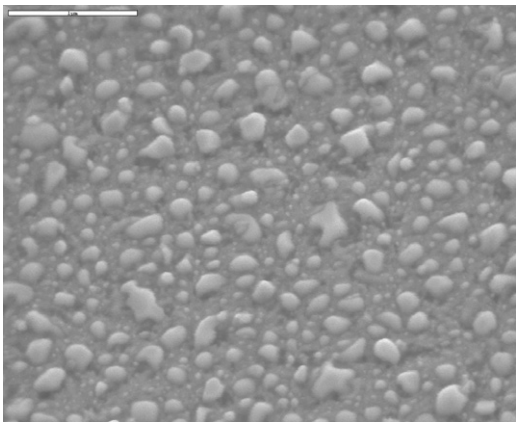

Figure 3. SEM image of a film grown under vacuum at 700 °C (scale bar 1 μm).

rough surface morphology deduced from the RBS spectrum and which was observed by SEM analysis.

The oxygen pressure during the growth plays an important role in the film composition. While at relatively high oxygen pressure (0.1 mbar) stoichiometric films are formed with uniform in-depth distributions, at 10^{-6} mbar and 700 °C, the RBS spectrum shows (figure 2(a)) a well defined Sn surface peak, while the other cationic elements are shifted to lower energies. This indicates the presence of an enriched Sn layer at the surface, while the bulk of the film is free of Sn. SEM analysis gave complementary details on the surface morphology of such films. Indeed, the presence of non-uniform particles with a molten aspect and various dimensions is evidenced in figure 3. Beneath the Sn rich surface layer, a mixed zirconium–titanium oxide layer is observed, with a Zr/Ti concentration ratio (0.88) different from that of the target (0.8).

Under the same low oxygen pressure and at room temperature the presence of this Sn rich layer is not observed (figure 2(b)). A uniform in-depth distribution for the cationic elements can be also deduced from this RBS spectrum, leading to an overall cationic composition, $Zr_{0.87}Sn_{0.23}Ti_{0.9}$, different from the target composition. In addition, the oxygen content of the films is also a function of the oxygen pressure during the growth. A decrease in the incorporation of oxygen into the films was evidenced by NRA; indeed the ratio of oxygen to overall cationic content was found to be around 1.8 in the low pressure domain (10^{-5}–10^{-6} mbar oxygen pressure). Oxygen vacancies are thus present in the zirconium titanate oxide films, a result similar to that obtained in the case of growth of another titanium based oxide [18].

The variations observed in the tin concentration in the ZST films as a function of oxygen pressure and temperature are related to the high volatility of the Sn species, i.e. due to its low evaporation temperature (298 °C); Sn desorption occurs for $T > 300$ °C under 10^{-6} mbar, but an increase in oxygen pressure allows the formation of SnO species at the surface of the growing film leading to incorporation of Sn in the film. Moreover, in order to explain the formation (at 700 °C under vacuum) at the film–substrate interface of a Zr–Ti oxide layer free from Sn under the Sn rich surface layer, we have to assume a high mobility for the Sn atoms in the films at elevated temperature (>400 °C), thus leading to Sn surface enrichment (figure 2(a)).

The drastic changes in the Zr/Ti ratio with the oxygen pressure and substrate temperature have to be related to processes that may act simultaneously during laser ablation. In fact, since Zr and Ti are not volatile species, the variations of the Zr/Ti ratio are due to the fact that Zr and Ti have different sticking coefficients which could change in the presence of oxygen atoms

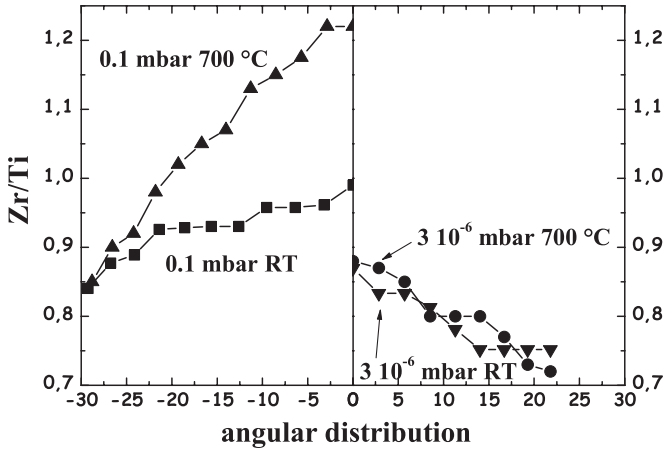

Figure 4. Angular distribution of the Zr to Ti concentration ratio as a function of temperature (room temperature and 700 °C) and oxygen pressure (0.1 and 10^{-6} mbar).

and as a function of temperature. Indeed, during laser ablation the plasma dynamics changes from a free expansion at 10^{-6} mbar to a collision dominated process in the presence of oxygen gas. The collisions between the species emitted by the target and the atoms or molecules of the gas will have two consequences. First these collisions will slow down the Zr and Ti species, and as the sticking coefficient could depend on the kinetic energy of the species variations in composition could be expected. Secondly, these collisions will broaden the angular distribution of the plasma. This broadening could be different for the various elements, and this will lead to differences in the lateral concentration ratio of these elements, as has been already observed in the case of PLD of complex oxides [17].

To check this last point, the angular distribution of the Zr and Ti elements was determined in the film as a function of the angle between the normal to the target and the position in the film. The results are presented in figure 4, with the Zr to Ti concentration ratio measured for various experimental conditions. These curves evidence differences in the broadening of the cation distribution according to the mass of the species. Indeed, this figure shows a decrease in the Zr content in the film with increasing angle to the normal. Whatever the growth conditions, the angular distribution of the Ti species is larger than that of Zr. For growth under a vacuum, this effect is due to collisions between atomic species in the plasma during its expansion. In a classical approach, during a collision between Zr and Ti, the species with the lighter mass (Ti) deviate more than the other (Zr), leading to the differences observed in figure 4. This difference in angular broadening is more pronounced under high oxygen pressures due to the additional collisions between species of the plasma and oxygen molecules from the ambient gas.

Two extreme domains can thus be defined in the growth of ZST thin films. At high oxygen pressure ($>10^{-3}$ mbar) and temperature (700 °C), homogeneous, uniform and almost stoichiometric film formation occurs. In these conditions, films with a rather smooth surface are obtained, and desorption of Sn from the film surface is depressed in this 10^{-3}–0.1 mbar range, i.e. the Sn component with a low melting point is prevented from evaporating from the surface. At low oxygen pressure, Sn desorption leads to a two-layer structure with an oxygen deficient Zr–Ti oxide near the substrate covered by a non-uniform layer of Sn oxide, as shown by the SEM measurements presented in figure 3. Between these two extreme cases, a non-uniform depth distribution of Sn in the films was observed.

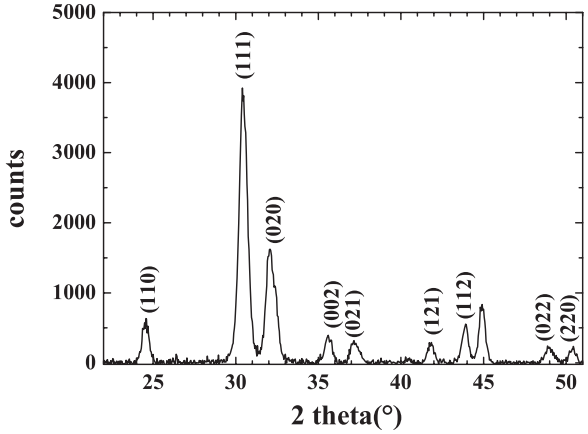

Figure 5. Grazing incidence x-ray diffraction diagram for ZST films grown on Si substrate at 700 °C under 10^{-2} mbar oxygen pressure.

Table 1. Lattice parameters of the orthorhombic phases of ZrSnTiO and ZrTiO bulk material.

$Zr_{0.8}Sn_{0.2}TiO_4$	$ZrTiO_4$
Orthorhombic phase	Orthorhombic phase
$a = 0.478$ nm	$a = 0.478$ nm
$b = 0.553$ nm	$b = 0.547$ nm
$c = 0.505$ nm	$c = 0.503$ nm

Table 2. Lattice parameters for ZST films grown at 700 °C under various oxygen pressures on Si and MgO single crystal substrates. The values for number of units of ZST in coincidence with units of MgO for domain matching epitaxy are also given.

	10^{-1} mbar	10^{-2} mbar	10^{-3} mbar	10^{-6} mbar
Si substrate	Orthorhombic $a = 0.482$ nm $b = 0.554$ nm $c = 0.505$ nm	Orthorhombic $a = 0.479$ nm $b = 0.552$ nm $c = 0.504$ nm	Orthorhombic $a = 0.479$ nm $b = 0.554$ nm $c = 0.504$ nm	Multiphased material
MgO substrate	Tetragonal $a = 0.492$ nm $c = 0.555$ nm	Tetragonal $a = 0.486$ nm $c = 0.554$ nm	Tetragonal $a = 0.496$ nm $c = 0.554$ nm	Cubic $a = 0.497$ nm
Domain matching epitaxy	6 units film 7 units MgO	13 units film 15 units MgO	11 units film 13 units MgO	11 units film 13 units MgO

3.2. Film structure

The crystallization of the ZST thin films was studied as a function of the growth conditions (oxygen pressure and laser fluence) and of the nature of the substrate (Si, MgO and sapphire). The XRD patterns obtained in grazing incidence geometry for ZST thin films grown on an Si substrate at 700 °C in the high pressure regime (10^{-2} mbar) are presented in figure 5. It is known that $Zr_{0.8}Sn_{0.2}TiO_4$, like $ZrTiO_4$, exhibits an orthorhombic crystal structure of the α-PbO type, and belongs to the *Pbcn* space group. The corresponding lattice parameters are given in table 1. The main reflection peaks observed in figure 5 can be identified with the main (*hkl*) planes of the classical orthorhombic structure, as indicated in the figure. The values of the lattice parameters deduced from these patterns are given in table 2 for the films grown under oxygen in the high pressure range ($>10^{-3}$ mbar). The slight differences in axis parameters can

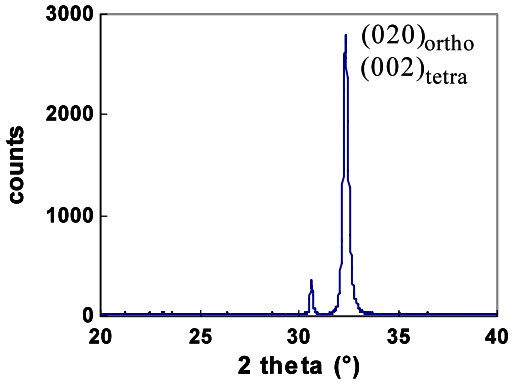

Figure 6. θ–2θ x-ray diffraction diagram for a ZST film grown on a MgO single crystal substrate at 700 °C under 10^{-2} mbar oxygen pressure.

be related to the change in the Sn concentration, and to the variation in the Zr/Ti ratio with film growth conditions.

An effect of the laser fluence on the crystallization of the ZST thin films was shown: a decrease in laser fluence increases the crystalline quality of the films, as indicated by the increase in peak intensity and the decrease of the peak width in the XRD patterns. In PLD, for a fixed laser wavelength the laser fluence determines the number of species emitted by the target at each laser pulse, and the kinetic energy of these species. An increase in laser fluence will thus increase the amount and energy of the species reaching the substrate. Combination of these two points induces a large structural disorder in the growing film. In PLD, a better crystallinity of the film is generally obtained by reducing the deposition rate, i.e. by decreasing the laser fluence.

The ZST films grown on Si substrates were polycrystalline, with a tendency to present a (111) preferred orientation as shown in the XRD patterns registered in the Bragg–Brentano geometry. This texture can be classically explained by surface energy considerations, i.e. as the (111) plane presents the lower surface energy [6, 9] growth occurs with these planes parallel to the substrate. Different results were obtained by using MgO single crystal as the substrate, as shown in figure 6 which represents an x-ray diffraction diagram in the Bragg–Brentano geometry for a film grown at 700 °C and 10^{-2} mbar in the high oxygen pressure domain. An intense peak is observed at a θ value of 32.4° and could be identified with the (020) peak of the ZST structure. The mosaic spread of this texture was studied by rocking curve measurements, and a rather large FWHM (2°) was observed, indicating a noticeable disorientation of the ZST crystallites with respect to the normal to the MgO substrate. Very similar results were obtained for films grown between 10^{-3} and 0.1 mbar, a second minor orientation (which could be ascribed to the (111) one, (see figure 6)) sometimes being observed. The films grown under the same experimental conditions on *c*-cut sapphire (001) substrates show the preferential growth of (110) and (111) ZST oriented crystallites with the orthorhombic structure. These results demonstrate the importance of the nature of the substrate on the crystalline orientation and quality of the films.

The (020) texture observed in ZST films grown on MgO single crystal substrate could suggest the epitaxial growth of such films. Pole figure measurements were thus carried out, and figure 7(a) represents a typical result for the (111) family planes. Four (111) poles are observed with a four-fold symmetry (each pole being located at 90° from the others), and with an azimuthal angle ψ of 57.5°. Such a pole figure should not be observed in the case of an orthorhombic structure for the crystallites oriented in the (020) direction. Indeed, in such a case, and according to the two possible in-plane orientations (related to the difference in

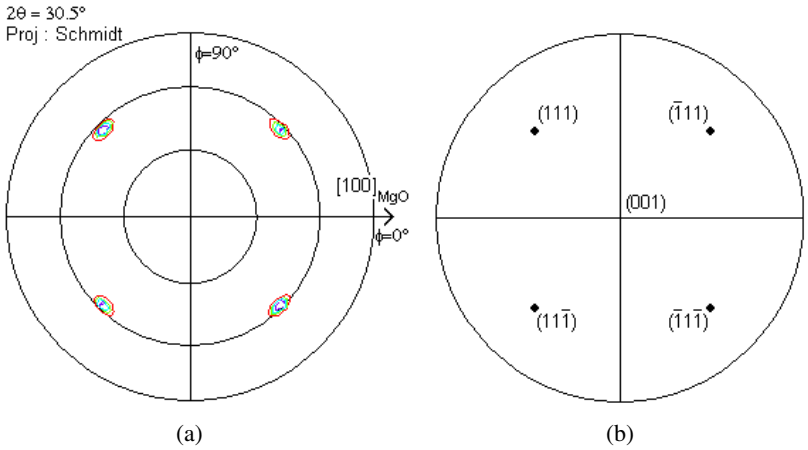

Figure 7. Pole figure of the (111) planes (a) for a ZST film grown (10^{-2} mbar, 700 °C) on MgO single crystal substrate and (b) simulation for a tetragonal structure.

the a and c axis parameters of the orthorhombic structure), two series of four poles should be observed. Precise measurements via two-axis (φ, ψ) scans around the poles observed in figure 7(a) indicate the presence of a single pole in each case. Such a result is clearly explained by a quadratic symmetry in the plane, i.e. the a and c axis parameters are equal, and a tetragonal structure is deduced. It has to be noticed that the diffraction peak at 32.4° in figure 6 corresponds to the (002) plane of this tetragonal phase. In what follows the planes and directions which are given are those of this tetragonal phase. The simulation of the stereographic projection of the (111) planes corresponding to this tetragonal structure is presented in figure 7(b), assuming that the [100] direction of the film and substrate are aligned.

From this analysis, the axis parameters measured for the films grown on MgO single crystal substrates in the high pressure regime are presented in table 2. The c axis parameter of this tetragonal phase is independent of the oxygen pressure, while the in-plane parameter shows measurable variations. This point is not yet explained, because changes in cationic composition and/or oxygen content of these films with the oxygen pressure should affect both the a and c axis parameters.

Concerning the formation of a tetragonal phase in this work, it has been reported that the replacement of 50% of Zr by Sn induces a morphotropic phase transition from orthorhombic towards a tetragonal (rutile) structure in bulk ZrSnTiO material [19]. However, the RBS analysis of these films indicates (figure 1(a)) that the Sn content in the films is very much lower (25%) than that leading to the stabilization of this tetragonal phase. The growth of this phase in the present work thus has to be related to the epitaxy stabilization effect [20, 21], i.e. the substrate, through the epitaxy, forces the growth in the ZST film of the crystalline phase having a structure coherent with its own structure. In this frame the precise in-plane orientation of the ZST film with respect to the substrate has to be discussed. Figure 7(b) shows that the following epitaxial relationship is obtained between the tetragonal ZST film and the cubic MgO substrate:

$$[100]_{\mathrm{ZrSnTiO}} \parallel [100]_{\mathrm{MgO}}.$$

Due to the large lattice mismatch between film and substrate (>13%), it is not possible to envisage a direct epitaxy with one unit of ZST in coincidence with one unit of MgO. A domain matching epitaxy [22, 23] which can explain the epitaxial growth of films on substrates with

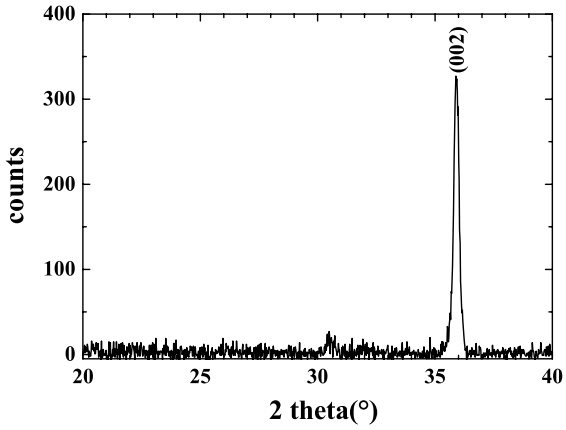

Figure 8. θ–2θ x-ray diffraction diagram for a ZST film grown on MgO single crystal substrate at 700 °C under 10^{-6} mbar oxygen pressure.

a large lattice mismatch has to be considered. In this case, m lattice units of the film will match with p lattice units of the substrate. With the values of in-plane lattice parameters for the ZST films grown in the high pressure domain, and MgO substrate (0.421 nm), the values of m (for ZST) and p (for MgO) leading to a lattice mismatch lower than 1% are given in table 2. The respective m and p values of the ZST units in coincidence with units of MgO are high, but such values are currently observed in the case of the growth of oxide films on oxide substrates [23]. Regarding the interface structure between film and substrate, one must note that in the growth conditions ($T > 400$ °C and limited oxygen pressure), the surface of the MgO should be described as an oxygen plane due to the surface rumpling phenomenon, i.e. the cations are displaced downwards, towards the bulk relative to the oxygen atoms [24]. This means that since the surface plane of MgO is negatively charged, the first atomic plane of the ZST should be a positively charged cationic plane. The epitaxial relationship would thus be defined by the domain matching epitaxy between a square lattice of oxygen and the cationic square lattice of the tetragonal ZST film.

In the case of ZST films grown on c-cut sapphire substrates which show (110) and (111) preferred orientations, pole figure measurements were carried out for the (111) and (020) family planes. Poles were not observed in these measurements. On the contrary, only rings showing a reinforcement in intensity were observed for the azimuthal ψ values expected for the orthorhombic phase. This means that the (110) and (111) textured crystallites do not present any in-plane orientation with the substrate, i.e. the ZST films grown on c-cut sapphire substrates are not epitaxial films.

The films grown at 700 °C under vacuum (10^{-6} mbar) on Si substrates, with an almost pure zirconium–titanium oxide at the film–substrate interface, were also crystalline, but it was not possible to identify their structure. In fact, the reflection peaks observed in the diffraction patterns for films grown on Si substrates could not be identified with those of the orthorhombic structure of $ZrTiO_4$. A multiphase material or a phase not previously reported could be envisaged. In the case of growth on MgO substrates, the analysis was more successful, and figure 8 represents the x-ray diffraction diagram recorded for a film grown in these conditions on an MgO single crystal. A single peak which could be identified as the (200) peak of the $ZrTiO_4$ orthorhombic phase, is present with a low intensity peak located around 30° and which could be identified as the (111) plane, while peaks due to a Sn oxide phase related to the surface islands were not observed. Such a diagram cannot precisely define the structure of the films, and additional insights were obtained by the pole figure of the (311) family planes which is presented in figure 9. This figure shows 16 distinct poles, four of which are marked on the

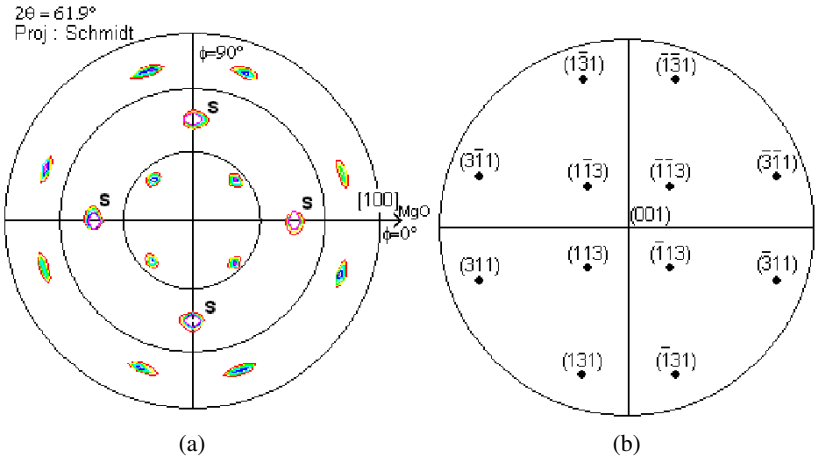

Figure 9. Pole figure of the (311) planes (a) for a ZST film grown (10^{-6} mbar, 700 °C) on MgO single crystal substrate, the poles corresponding to the (220) of the substrate are indicated by a 's' for substrate. (b) Simulation of the pole figure for a cubic structure.

figure and correspond to the (220) poles of the MgO single crystal substrate (their diffraction angle 2θ being close to that of the (311) family of the ZST film). The other two series of poles can be well described in the case of a cubic structure by the four poles of the (113) planes and the eight poles of the (311) and (131) planes, as shown on the simulation of the stereographic projection in figure 9(a) (obtained with the [100] direction of the film aligned with that of the substrate). It has to be noticed that a tetragonal structure should also give 12 poles, but in this case the diffraction angle 2θ of the (113) and (311) planes should be different from that of the (131) plane. Careful measurements of these diffraction angles for all the poles in figure 9(a) lead to a single value (61.9°) corresponding to an axis parameter of 0.497 nm for the cubic structure.

In addition, the poles observed in figure 9 characterize epitaxial growth of the film with the following in-plane orientation:

$$[100]_{\mathrm{ZrTiO}} \parallel [100]_{\mathrm{MgO}}$$

i.e. 'cube on cube' epitaxial growth. The lattice parameters of the film (0.497 nm) and substrate (0.421 nm) are such that the growth of the film with the lattice parameter of the substrate would lead to very high values of internal strain in the films (lattice mismatch = 16%), which preclude such a process. In the frame of domain matching epitaxy, a good coincidence can be obtained with 11 units of ZST matching with 13 units of MgO, leading to a lattice mismatch lower than 0.5%. However, as in the case of the film grown at 0.1 mbar oxygen pressure, this is just a geometrical approach and the precise in-plane orientation would be determined by energy considerations. In fact, the film–substrate interface energy has to be at a minimum, and in the case of ionic oxides the main contribution to the interface energy is related to the electrostatic interaction between the MgO plane (which would be an oxygen atomic plane) via the rumpling of the surface and ZST plane (which would be a positively charged cationic plane) at this interface, and the determination of this energy would be useful for explaining the in-plane orientation of the film.

The film at the surface of the substrate is a zirconium titanate oxide. Such a material in bulk form crystallizes in the orthorhombic structure (table 1), thus a question arises about the origin of the change of structure towards the cubic structure observed in this work. A solely

epitaxial stabilization effect [20] of this cubic phase appears questionable, taking into account the previous results observed in the high oxygen pressure domain (epitaxial stabilization of a tetragonal phase). The origin of this structural change has to be searched for in the growth conditions, i.e. the oxygen pressure seems to play an important role in the structural change: a tetragonal structure is obtained in the high oxygen pressure range and a cubic one in the low pressure domain. In the case of films grown under low oxygen pressure, the ratio of the oxygen to the overall cationic content was found around 1.8, as deduced from the NRA and RBS analyses. By comparison with the theoretical value of 2 corresponding to a stoichiometric zirconium titanate oxide, a large concentration of oxygen vacancies is present in such films. The presence of oxygen vacancies can induce an increase in the axis parameter in the oxide lattice, due to the severe Coulombic repulsion between the cations. This has been previously observed in the case of some titanium based oxides [18, 25]. However, a change in the crystal structure for titanium based oxides can be also envisaged. For example, in the case of $BaTiO_3$ it has been reported that oxygen non-stoichiometry ($BaTiO_{2.83}$) leads to a change of crystalline structure—from the cubic perovskite towards a hexagonal one [26]. In the same way, the cubic perovskite $PbTiO_3$ drastically changes towards other structural phases (pyrochlore phases), with a deficiency in oxygen [27]. The structural change from orthorhombic to cubic structure observed in this work could thus be related to the presence of an important concentration of oxygen vacancies in the ZST film grown under vacuum. This previously unobserved crystalline oxide phase is stable at room temperature, and this stability is certainly due to the fact that the Ti species can have different valency states (Ti^{4+} and Ti^{3+}) and can thus easily accommodate the presence of oxygen vacancies [18].

3.3. Optical properties

The optical properties of almost stoichiometric ZrSnTiO films grown in the high oxygen pressure domain were studied by spectroscopic ellipsometry. First the thicknesses and refractive indices of the films were determined in the 1.6–3 eV range using the Cauchy dispersion law to model the optical response of the ZST layer. The optical constants of the substrates were taken from handbooks. A surface layer was added to the model, to take into account an eventual surface roughness of the films. Its optical properties were modelled by a Bruggeman effective medium mixing the indices of the ZST layer and those of vacuum with a volume fraction of 50%. Then the complex dielectric function $\varepsilon = \varepsilon_1 + i\varepsilon_2$ of ZrSnTiO was extracted wavelength by wavelength in the whole spectral range using the structure defined in the preceding step.

Figures 10(a) and (b) present the dielectric function of the films grown on Si substrates as function of the deposition temperature. In the case of the ZST film grown at 700 °C, the surface layer was not necessary to obtain a good fit, while the dielectric function of the film grown at room temperature could be almost perfectly described by a mixture of the indices of the layer grown at 700 °C and with 70% voids. This is indicative of a large porosity in the film grown at room temperature on Si substrates, in agreement with the RBS results (figure 1(b)).

Figure 11(a) and (b) present a comparison of the dielectric functions of the layers grown at 700 °C on Si, MgO and Al_2O_3 substrates. A clear maximum in ε_2 near 5.2 eV was observed for the ZST layers grown on MgO and Al_2O_3 substrates as compared to Si substrates. Two facts could be related to this observation. First the films grown on Si substrates present a worse crystalline quality with respect to the films grown on MgO or Al_2O_3 single crystal substrates, and secondly the crystalline structures are different (orthorhombic and tetragonal).

Figure 12 presents a Tauc plot of the absorption coefficient α of the layers. The extrapolation to zero of the linear part of the curve gives the position of the Tauc band gap.

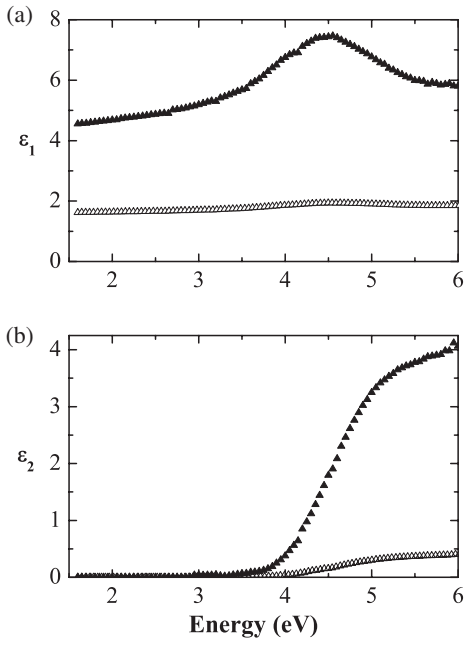

Figure 10. Real (a) and imaginary (b) parts of the dielectric function of two ZST films grown under 10^{-1} mbar O_2 on Si substrates at 700 °C (triangles) and RT (open triangles). Despite the apparent large differences, the dielectric function of the film grown at RT is similar to that of the film grown at 700 °C mixed with voids.

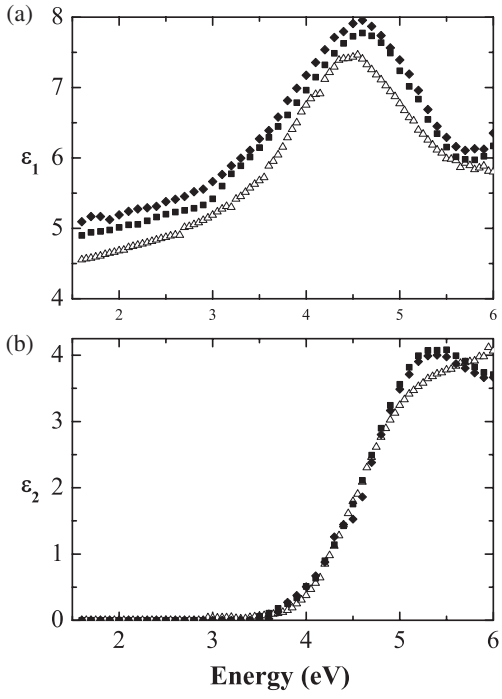

Figure 11. Real (a) and imaginary (b) parts of the dielectric functions of ZST films grown at 700 °C under 10^{-1} mbar O_2 on Si (open triangles) Al_2O_3 (diamonds) and MgO (squares) substrates.

The layers deposited on Al_2O_3 and MgO had a band gap of 3.5 eV. For the layer deposited on Si, the band gap was estimated at 3.6 eV. However, owing to the dispersion in the values of the absorption coefficient the 0.1 eV change in the position of the band gap may not be significant. An Urbach tail, with an Urbach energy of 250 meV, was observed below the band gap of the

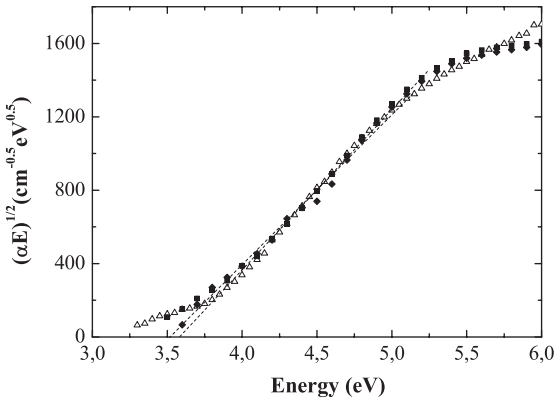

Figure 12. Tauc plot of the absorption coefficient α of ZST films grown at 700 °C under 10^{-1} mbar O_2 on Si (open triangles) Al_2O_3 (diamonds) and MgO (squares) substrates. The dotted lines present linear approximation of $(\alpha E)^{1/2}$.

ZST layer deposited on Si. All the layers deposited at 700 °C had an optical band gap, given at $\alpha = 10^4$ cm^{-1}, near 3.7 eV.

The band gaps of $ZrTiO_4$ films have been determined on silica substrates from transmittance measurements analysed using a dispersion law [28]. The value of the Tauc band gap was found to be nearly 3.5 eV, and varied only slightly depending on the deposition temperature, and hence on crystallinity. Our results are in good agreement with those of [28] concerning the value of the band gap and its weak evolution with crystallinity. The band gap of $Zr_{0.8}Sn_{0.2}TiO_4$ layers has been determined from ellipsometric measurements using a Cauchy dispersion law [6]. A band gap value of 3.3 eV was obtained using the Tauc formula. The value of the band gap determined in our work is larger. However, using the Cauchy dispersion law [6] leads to a poor sensitivity to the real value of the band gap, and the composition of our films is different from $ZrTiO_4$. In addition we observed an Urbach tail in the absorption of layers deposited on Si substrates which was indicative of disorder in the atomic positions or bonds angles. This may suggest that the layers were less crystallized on Si substrate as compared to the Al_2O_3 and MgO substrates.

4. Summary

The presence of a volatile species (Sn) in the ZrSnTiO material, the variation of the sticking coefficient of the elements with substrate temperature and oxygen pressure and the broadening of the angular distribution of the species during plume expansion are the main difficulties in the formation of ZrSnTiO thin films by PLD. This study leads to a determination of the growth conditions for the formation of stoichiometric, dense ZrSnTiO films with a good crystalline quality and a rather smooth surface, i.e. $T > 600$ °C in the 10^{-3}–10^{-1} mbar oxygen pressure range. Lower oxygen pressures lead to large losses of Sn and the formation of a two-layer system with an understoichiometric zirconium titanate oxide layer covered by a non-uniform SnO_x surface layer.

Previously unobserved crystalline phases were identified in the ZST films. First a tetragonal structure is obtained in ZST films grown in the high oxygen pressure regime ($>10^{-3}$ mbar). This structural phase is certainly stabilized by epitaxy on MgO single crystal. This structural phase is perfectly stable at room temperature, and has never been observed in bulk material with the Sn concentration of the films grown in this work. In the case of films grown under a vacuum (10^{-6} mbar), the Zr–Ti oxide formed at the film–substrate interface presents a cubic structure which to the best of our knowledge has never before been reported

in bulk $ZrTiO_4$ material. This cubic oxide phase seems to be due to the reducing conditions of growth leading to the formation of an oxygen deficient phase with a high concentration of oxygen vacancies.

5. Conclusions and perspectives

As the optical properties of the ZST films were found to depend upon the crystalline quality of the films, the dielectric properties of such films epitaxially grown on MgO have to be studied to look at the effect of the change in crystalline structure on the dielectric constant. Works are now in progress to investigate the physical properties of this new tetragonal phase. Moreover, the high concentration of oxygen vacancies in the films grown at low oxygen pressure indicates the presence of Ti^{4+} and Ti^{3+} species in this phase. This would mean that these films could present interesting electronic transport properties, like those observed in understoichiometric Ti based oxides, and this will be studied in the near future.

References

[1] Wilk G, Wallace R and Anthony J 2001 *J. Appl. Phys.* **89** 5243
[2] Hirano S, Hayashi T and Hattori A 1991 *J. Am. Ceram. Soc.* **74** 1320
[3] Ioachim A, Toacsan M I, Banciu M G, Nedelcu L, Stoica G, Annino G, Cassettari M, Martinelli M and Ramer R 2003 *J. Optoelectron. Adv. Mater.* **5** 1395
[4] van Dover R B, Schneemeyer L F and Fleming R M 1998 *Nature* **392** 162
[5] Hsu C S and Huang C L 2004 *J. Appl. Phys.* **96** 1186
[6] Cheng W X, Ding A L, Qiu P S, He X Y and Zheng X S H 2003 *Appl. Surf. Sci.* **214** 136
[7] Hsu C S and Huang C L 2006 *Thin Solid Films* **498** 271
[8] Mays E L, Hess D W and Rees W S Jr 2004 *J. Cryst. Growth* **261** 309
[9] Nakagawara O, Toyota Y, Kobayashi M, Yoshino Y and Katayama Y 1996 *J. Appl. Phys.* **80** 388
[10] Lu X B, Wang Y P, Ling H Q and Liu Z G 2002 *J. Non Cryst. Solids* **303** 88
[11] Viticoli M, Padeletti G, Kaciulis S, Ingo G M, Pandolfi L and Zaldo C 2005 *Mater. Sci. Eng.* B **118** 87
[12] Nistor M, Gherendi F, Magureanu M, Mandache N B, Iochim A, Banciu M G, Nedelcu L, Popescu M, Sava F and Alexandru H V 2005 *Appl. Surf. Sci.* **247** 169
[13] Chrisey D B and Hubler G K (ed) 1994 *Pulsed Laser Deposition of Thin Films* (New York: Wiley)
[14] Morcrette M, Gutierrez-Llorente A, Seiler W, Perrière J, Laurent A and Barboux P 1999 *J. Appl. Phys.* **88** 5100
[15] Doolittle L R 1985 *Nucl. Instrum. Methods* B **9** 344
[16] Schmaus D and Vickridge I 2005 *Analytical Methods for Corrosion Science and Engineering* ed P Marcus and F Mansfeld (New York: Dekker) Chapter 6 (MeV Ion Beam Analytical Methods)
[17] Gonzalo J, Afonso C N and Perrière J 1995 *Appl. Phys. Lett.* **67** 1325
[18] Morcrette M, Gutierrez-Llorente A, Laurent A, Perrière J, Barboux P, Boilot J P, Raymond O and Brousse T 1998 *Appl. Phys.* A **67** 425
[19] Watino K, Minai K and Tamura H 1984 *J. Am. Ceram. Soc.* **67** 278
[20] Kaul A R, Gorbenko O Yu, Grabov I E and Samoilenkov S V 2002 *Crystal Growth in Thin Solid Films* ed M Guilloux-Viry and A Perrin (India: Research Signpost) p 255
[21] Gorbenko O Yu, Samoilenkov S V, Grabov I E and Kaul A R 2002 *Chem. Mater.* **14** 4026
[22] Narayan J, Dovidenko K, Sharma A K and Oktyabarsky S 1998 *J. Appl. Phys.* **84** 2597
[23] Narayan J and Larson B C 2003 *J. Appl. Phys.* **93** 278
[24] Alfonso D R, Snyder J A, Jaffe J E, Hess C A and Gutowski M 2000 *Phys. Rev.* B **62** 8318
[25] Hiratani M, Imagawa K and Takagi K 1995 *Japan. J. Appl. Phys.* **34** 254
[26] Woodward D I, Reaney I M, Yang G Y, Dickey E C and Randall C A 2004 *Appl. Phys. Lett.* **84** 4650
[27] Gelabert M C, Laudise R A and Riman R E 1999 *J. Cryst. Growth* **197** 195
[28] Chang D A, Lin P and Tseng T Y 1995 *J. Appl. Phys.* **77** 4445